

# Role of Cardiac MRI in Pulmonary Hypertension



Ravi Desai, MD



Fernando Torres, MD



Himanshu Gupta, MD

Ravi Desai, MD<sup>1</sup>  
Fernando Torres, MD<sup>2</sup>  
Himanshu Gupta, MD<sup>1\*</sup>

<sup>1</sup>Department of Medicine,  
Division of Cardiovascular Disease  
University of Alabama at Birmingham  
Birmingham, AL

<sup>2</sup> Department of Medicine,  
Division of Pulmonary and  
Critical Care Medicine,  
University of Texas  
Southwestern Medical Center  
Dallas, TX

Pulmonary hypertension (PH), a disorder characterized by abnormally elevated blood pressure in the pulmonary circulation and increased pulmonary vascular resistance, is classified into five diagnostic categories: pulmonary arterial hypertension (PAH), PH with left-sided heart disease, PH associated with lung disease and/or hypoxemia, PH due to chronic thrombotic and/or embolic disease, and a miscellaneous group.<sup>1</sup> Right-sided heart catheterization (RHC) is the current reference standard for the diagnosis and assessment of the severity of PH.<sup>2,3</sup> However, this invasive technique may not be suitable for repeated studies, such as monitoring the time course of functional recovery. Echocardiography including doppler assessment of tricuspid and pulmonary valves offers a well established, bedside assessment of PH.<sup>4</sup> Despite advances in echocardiographic techniques, it is often not feasible to obtain a comprehensive and integrated evaluation of the right ventricular structure and function, or the pulmonary vascular system.

Additional imaging techniques are often necessary to define the etiologic mechanisms and the severity of PH, information important to individualize the management strategies and to accurately assess prognostic parameters. Out of these techniques, cardiac magnetic resonance imaging (cMRI) has become an important diagnostic tool for the comprehensive evaluation of PH. Due to its ability to not only assess the right ventricular mechanics but also evaluate pulmonary circulation and other structural abnormalities in 3-dimensional projections, cMRI is expected to play an increasingly important role in the diagnosis and management of PH. In this review article we summarize the present status of cMRI in PH and discuss some emerging applications in PH.

## Overview of Cardiac MRI (cMRI)

MRI is an elegant noninvasive technique free of ionizing radiation that uses a powerful magnetic field to align the spin of pro-

*Key Words*—pulmonary hypertension; magnetic resonance imaging (MRI).  
Address for reprints and other correspondence: Himanshu Gupta, MD,  
University of Alabama at Birmingham, BDB-101, CVMRI, 1808 7th Ave.  
South, Birmingham, AL 35294; email: hgupta@uab.edu.

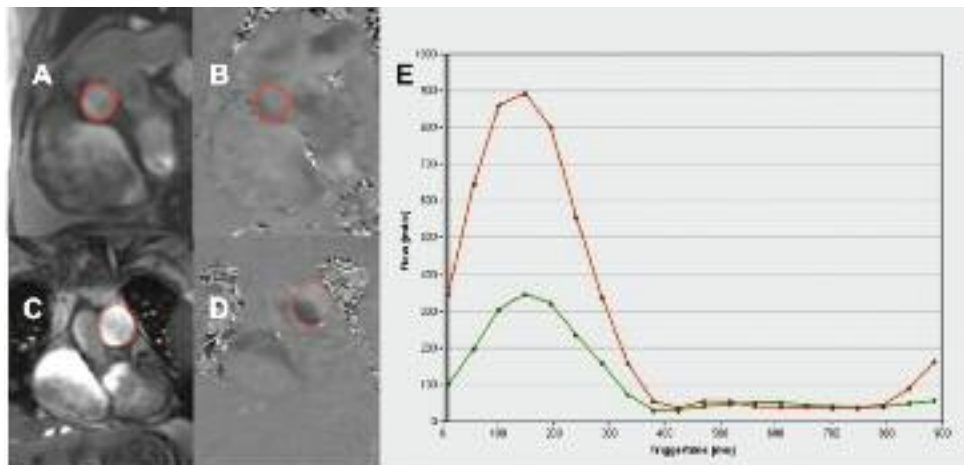


**Figure 1.** Phase contrast (PC) imaging for the quantification of stroke volume and shunt. A and B show the modulus and phase image respectively for measuring aortic flow. Cross-section of ascending aorta is encircled in solid contour. C and D show the modulus and phase image respectively for measuring the main pulmonary artery flow. Cross-section of proximal main pulmonary artery is encircled in dashed contour. Flow curves are depicted in E. Main pulmonary artery flow (top curve) was calculated as 223ml/beat and aortic flow (bottom curve) was 97 mL/beat with resultant Qp/Qs ratio of 2.3

tons followed by a brief radiofrequency (RF) pulse to perturb the steady state of these protons. A signal is generated when the individual protons return towards their steady state that can be used to generate images in any anatomical plane. Although MRI has been extensively used to evaluate structures such as brain, the application to cardiac imaging was hampered due to motion caused by cardiac cycle and respiration. Development of cMRI has been exponential with techniques of cardiac and respiratory gating, fast gradient-echo techniques, segmented k-space allowing a single breath hold scan, echo sharing and more recently novel methods of k space filling and parallel imaging. A brief summary of basic techniques useful in cardiac MRI is summarized below.<sup>5</sup>

## Black-blood anatomical imaging

In this imaging method, the flowing blood gives no signal. Therefore this is called 'black-blood' technique. The signal in this technique is dependent on the same proton experiencing both 90 degree and 180 degree RF pulses. Therefore the flowing blood protons do not give any signal; in contrast other structures such as myocardium appear bright. Today, black blood imaging is used for specific applications involving structural abnormalities of the ventricles and evaluating the pericardium (**Figure 1A**).

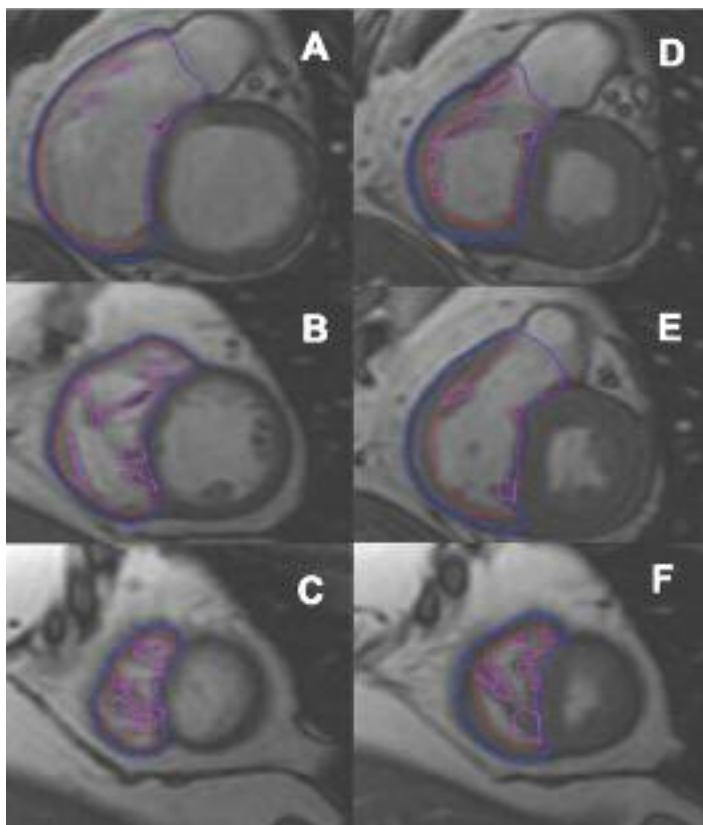


**Figure 2.** Right ventricular volumes, mass and ejection fraction. Selected short axis slices (steady state free precession sequence, a bright blood technique) in end-diastolic phase (A, B, C) and end-systolic phase (D, E, F) are shown with epicardial and endocardial contours. Contours around the papillary muscles and trabeculations are also drawn. The summed volume enclosed by endocardial contour is calculated for measuring total ventricular volume in end-diastole and end-systole respectively. Myocardial mass is measured as a difference of the endocardial and epicardial volumes multiplied by specific gravity of the myocardium.

### Cardiac Cine imaging using bright blood technique

Currently Cine MR with steady state free precession is the workhorse of functional imaging. It uses T2 effects to generate bright blood images and segmented k space with echo sharing to achieve multiple cardiac phases (typically 20) of a single slice in one breath hold time. There is excellent blood-myocardial contrast that makes ventricular volume and myocardial mass measurements extremely accurate (Figures 2, 3, and 4B). Techniques of parallel imaging and non-cartesian k-space sampling has shortened the acquisition time to a point where it is now possible to obtain images in real time without cardiac gating and breath holding.

### Myocardial tagging

Myocardial tagging refers to a family of techniques that lay out a saturation grid or series of saturation lines across the heart. Deformations of these lines due to myocardial contraction are then monitored. When combined with cine imaging, tagging can be used to measure myocardial strain in three dimensions. Currently as a research tool, it has extensive application in the study of cardiac mechanics (Figure 3D).

### Flow quantification (Phase contrast MRI)

One of the attributes of the MR signal is that its phase can be used to encode flow information. Therefore hemodynamic information similar to doppler imaging can be obtained. This tech-

nique can be extremely useful for shunt quantification and calculating stroke volumes/ cardiac output. (Figure 4).

### Myocardial viability imaging: Delayed contrast enhancement.

The technique for delayed enhancement MR imaging involves intravenous infusion of gadolinium chelate contrast material (0.1–0.2 mmol/kg) followed 10–30 minutes later by a cardiac-gated T1-weighted pulse sequence. There is altered wash-in and wash-out kinetics of the MRI contrast agent in acute necrosis and chronic scar as compared to the un-affected myocardium. Using inversion recovery sequence, it is possible to select inversion time in such a way that there is no signal from viable myocardium. The scar tissue therefore appears bright on this technique. This technique is extremely accurate in evaluating myocardial fibrosis. However this technique is not used as first line imaging modality in patients with renal insufficiency due to risk of nephrogenic systemic fibrosis (NSF).

### MR angiography of pulmonary arteries

Contrast enhanced magnetic resonance angiography (MRA) can be used to evaluate pulmonary arteries and veins. Major advantage of MRI is its ability to assess pulmonary arteries where CT may be contraindicated. Due to recent concerns of NSF in patients with renal insufficiency, use of this technique has been relegated to those patients with contrast allergy. Non-contrast gradient or spin echo based techniques can also be used to evaluate pulmonary arteries in the proximal segments.

## cMRI in the Diagnosis and Assessment of Pulmonary Hypertension (PH)

### Assessment of right ventricular volumes, mass and function

In response to pressure overload by PH, there is compensatory right ventricular (RV) myocardial hypertrophy<sup>6</sup> followed by progressive contractile dysfunction, chamber dilatation and finally clinical evidence of decompensated right ventricular failure characterized by rising filling pressures and diminishing cardiac output, which is compounded by tricuspid regurgitation due to annular dilatation and poor leaflet coaptation. Thus, the function and size of the right ventricle is not only an indicator of the severity and chronicity of pulmonary hypertension but also imposes an additional cause of symptoms and reduced longevity. Right ventricular function appears to be the most important determinant of life expectancy in patients with pulmonary arterial hypertension.<sup>7-9</sup> A trend of increasing RV volume and decreasing stroke volume and LV volume are strong predictors of mortality and treatment failure. Therefore, accurate assessment of RV structure and function is extremely important in the evaluation and serial follow-up of PH. Unlike the left ventricle (LV), which can be reasonably modeled as a symmetric ellipsoid, the RV is crescent-shaped in cross section and triangular when viewed laterally. MRI with its high spatial and temporal resolution along with 3-dimensional imaging capabilities is considered the “gold standard” in functional assessment of right ventricle.<sup>10-12</sup> MRI demonstrates good inter-study reproducibility for RV function parameters in healthy subjects, patients with heart failure, and patients with hypertrophy<sup>13</sup>. RV mass which is otherwise difficult to measure noninvasively can be accurately quantified with MRI with good reproducibility (Figure 2).<sup>13</sup>

### Assessment of Interventricular septum

The interventricular septum is normally bowed to the right. In all

the cardiac phases of a short axis imaging, the left ventricle maintains a circular shape while the right ventricle keeps a crescent shape. In the presence of right ventricular pressure overload, the septum flattens or even bulges to the left in early diastole causing a crescent shape of the left ventricle. This was classically believed to result from a negative inter-ventricular pressure gradient between the left and right ventricle during diastole, as suggested by studies using M-Mode echocardiography and hemodynamics.<sup>14</sup>

Tagged MRI study has shed more light on the mechanism behind this paradoxical septal motion. Maximal septal bowing towards left ventricle coincided with peak RV shortening and overstretch of septal wall. The overstretch (positive strain) indicates that the paradoxical septal motion is a result of higher pressure in the RV than in the LV, owing to the ongoing shortening in the RV free wall, whereas the LV free wall is already in its relaxation phase (Figure 3).<sup>15</sup>

### Noninvasive estimation of Right ventricular systolic pressure

During the cardiac cycle, the position of the interventricular septum (IVS) is primarily determined by the difference in pressure between the LV and the RV—that is, the transeptal pressure gradient. Similarly, the configuration of the LV free wall is determined by the difference between the LV pressure and the surrounding pressure—that is, the effective distending transmural pressure. In the absence of asymmetric hypertrophy, the wall stress in the IVS and in the free wall may be assumed to be similar; thus, any change in the dP ratio (ie, transeptal pressure gradient divided by effective distending transmural pressure) should affect the curvature ratio Rc (ratio of curvature of the IVS and curvature of the LV free wall) proportionally. Dellegrottaglie and colleagues<sup>16</sup> compared Rc and right ventricular systolic pressure (RVSP) by right heart catheterization (RHC). They showed a good correlation ( $r = 0.85$ ) and derived a formula for noninvasive calculation of RVSP as  $RVSP = SBP \cdot [1 - (R_c/1.03)]$ .

Laffon and colleagues<sup>17</sup> developed a computerized algorithm for estimating mPAP based on an MRI assessment of physical parameters (e.g., pulmonary artery cross-sectional area, blood flow velocity) that is weighted using patient-specific biophysical parameters (e.g., height, weight, heart rate). When this algorithm was applied to a series of 31 patients undergoing RHC, the calculated mPAP based on MRI-derived parameters correlated strongly with catheterization-derived values ( $r = 0.92$ ). In contrast to these generally positive results, Roeleveld and colleagues<sup>18</sup> assessed 44 patients with established PAH and found poor correlation between catheterization-derived mPAP and 5 different MRI-derived measures, including pulmonary vascular index, acceleration time (defined as time from onset of PA forward flow to maximum velocity), the ratio between acceleration time and ejection time, and the Laffon algorithm discussed previously. The only significant correlation between catheterization-based mPAP and MRI-based measures was for ventricular mass index ( $r = 0.56$ ,  $P < .001$ ). However, using a ventricular mass index cutoff of  $> 0.6$  to define PAH (as suggested by Saba and colleagues<sup>19</sup>) would result in a missed diagnosis in 9 patients, a false-negative rate of 20%. The investigators therefore concluded that at present, MRI-derived measures may be reasonable for use in screening and differential diagnosis; however, they are not yet capable of replacing right-heart catheterization in confirming PAH diagnosis.

### Phase contrast MRI (PC-MRI) derived flow parameters

Analysis of PC-MRI images involves automatic tracing of main PA

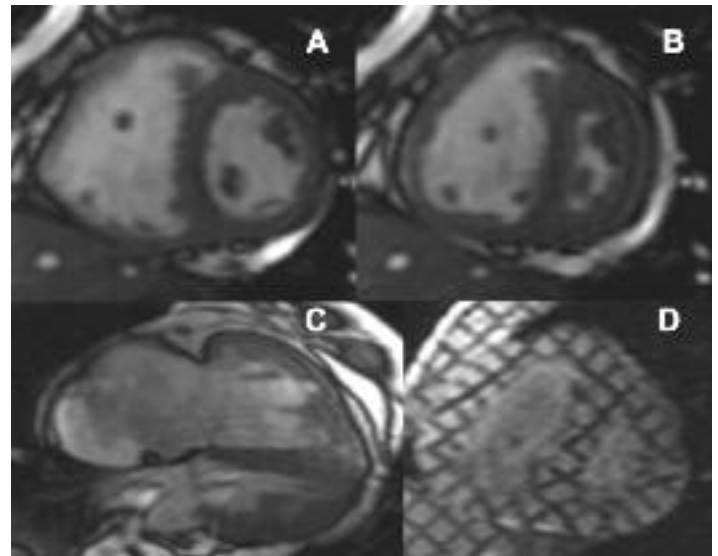


**Figure 3.** Changes in right ventricle and interventricular septum in PH short axis views of the ventricles (A and B) show dilated and hypertrophied right ventricle. The interventricular septum is bulging towards left ventricle in end-systole/ early diastole suggestive of right ventricular pressure overload. (C) Shows 4-chamber view of the heart with presence of pericardial effusion (\*), which is a poor prognostic sign in pulmonary hypertension. (D) Shows myocardial tagged images of the short axis views of the ventricle. These tagged images are used to derive strain and shear measures of cardiac mechanics.

contours with manual correction if necessary on magnitude and phase images of all phases. Using specialized post-processing software one can obtain velocity information for each pixel within the contour which when integrated over time, yields the following parameters: peak velocity, average velocity, and minimum, maximum, and average areas. PA strain or distensibility is calculated as  $100 \cdot (MaA - MiA)/MiA$ , where MaA is maximum pulmonary artery cross-sectional area and MiA is the minimum pulmonary artery cross-sectional area.

By using flow values at each time point, the following additional parameters are quantified: acceleration time (AT), ejection time (ET), and AT/ET ratio. AT is defined as the time interval from the beginning of the anterograde flow upslope in systole to the peak systolic flow. ET was defined as the interval from the beginning of the systolic flow upslope to the horizontalization of the flow curve, presence of a new upslope, or crossing of the zero-flow line during protodiastole.

Sanz and colleagues<sup>20</sup> compared the above parameters with RHC derived parameters and showed the average velocity of PA flow and minimum PA area as useful parameters to reveal PAH (area under receiver operating characteristic curve = 0.90 for average velocity and = 0.95 for minimum PA area). This strong correlation between average blood velocity and pulmonary pressures and resistance might allow noninvasive diagnosis of PAH. Using velocity-encoded cine-MRI, Kondo and colleagues<sup>21</sup> have shown that there is a reduced peak systolic velocity and greater post-systolic retrograde flow in the pulmonary arteries of PAH patients; retrograde flow was proportional to pulmonary resistance and inversely proportional to flow volume. In a recent study of 25 patients with PAH,<sup>22</sup> mean pulmonary artery (PA) peak flow velocity, PA blood flow, and PA distensibility were found to be significantly lower than in a matched group of volunteers ( $P = .002$ ,  $P = .002$ , and  $P = .008$ , respectively).

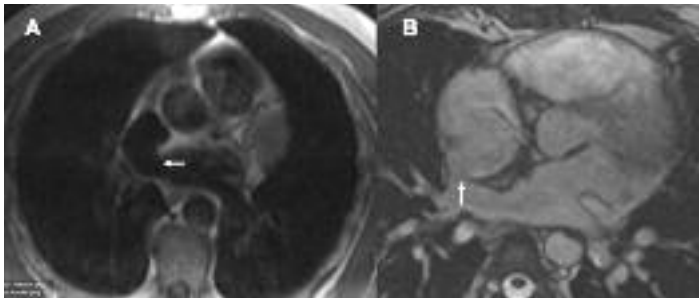


**Figure 4.** Sinus venosus atrial septal defect. (A) shows spin echo axial slice (a black blood technique) and (B) shows steady state free precession sequence axial slice of a patient with pulmonary hypertension. Arrow in the figure depicts the communication between left atrium and right atrium at the junction with superior vena cava diagnostic of sinus venosus atrial septal defect.

### Delayed contrast enhancement (DCE)

Contrast-enhancement techniques have revealed important cardiac structural abnormalities among patients with PAH. Blyth KG and colleagues<sup>23</sup> showed zones of DCE in 23 of 25 PAH patients. In 7 patients, DCE was confined to the RV insertion points, whereas in the remaining 16 patients, DCE extended from the insertion points into the interventricular septum. These zones likely corresponded with areas of mechanical stress (although mechanical stress has not definitively been shown to be the cause), suggesting that elevated RV pressures may lead to tissue abnormalities in these areas. All 16 of the patients in whom DCE was found in the interventricular septum also showed abnormal septal wall bowing (toward the LV during late RV systole). The DCE was also observed in a study conducted in 15 patients with PAH.<sup>24</sup> The extent of the DCE of the myocardium was inversely related to measures of RV systolic function (ie, RV ejection fraction [ $r = -0.63$ ,  $p = .001$ ], RV stroke volume [ $r = -0.67$ ,  $P = .006$ ], and RV end-systolic volume index [ $r = -.51$ ,  $P = .005$ ]).

### Right ventricular diastolic function

Isovolumic relaxation time (IVRT) may be a marker of RV diastolic function and correlates positively with both RV mass and pulmonary vascular resistance, parameters that are known to be of critical importance in the evaluation and prognosis of PAH.<sup>25-26</sup> One is also able to derive RV filling rates based on volume-time curves to assess early RV filling rate (E) and late RV fill rate (A). In PH patients, E is reduced when compared to control subjects, and toward end-diastole A is higher and shows a significant atrial contribution.<sup>25</sup>

### Chronic thromboembolic pulmonary hypertension (CTPH)

PAH is a complex disease that affects the right-sided circulation, by obliterative remodeling in the vascular wall, characterized by increased cellular proliferation and suppressed apoptosis.<sup>27</sup> This in turn leads to elevated pulmonary vascular resistance, increased RV afterload, RV failure, and premature death. By contrast, in CTPH there is progressive worsening of PH with time due to local thrombosis as a result of low blood flow upstream from the obstructed pulmonary artery, recurrent thromboembolism and remodeling of small distal pulmonary arteries. The blood clot gets organized into fibrous tissue with pseudo-intimal fibrous thickening that usually starts at the level of the intrapericardial segment of the pulmonary artery and becomes progressively thicker downstream in lobar and segmental arteries that eventually become occluded.<sup>28</sup> Pulmonary

endarterectomy is the treatment of choice in CTPH while PAH is managed medically. Accurate diagnosis is therefore essential.

A prerequisite for the correct and reliable diagnosis of CTPH is the depiction of occluding thrombotic material and concomitant perfusion defects. Until recently, pulmonary perfusion could be assessed only by using radionuclide perfusion scintigraphy and conventional pulmonary angiography. While the former has substantial limitations with respect to spatial and temporal resolution, the latter requires invasive catheterization of the right side of the heart. Also, conventional angiography is limited to two-dimensional projection images. A lung perfusion performed in PH does not reveal the severity of the disease, the prognosis or predict the response to various types of therapy.<sup>29</sup> Multi-detector computed tomography is increasingly being used as the initial diagnostic test for evaluation of CTPH.

Use of cMRI for CTPH is limited in application and scope due to number of technical challenges. Advent of parallel imaging techniques in MRI has made possible a nearly isotropic voxel with spatial resolution comparable to multi-detector CT<sup>30</sup> with additional capability of MR perfusion imaging. In a recent study, MR perfusion imaging and MR angiography alone showed good results in the differentiation of PAH and CTPH, enabling the correct diagnosis of PAH and CTPH in 69% and 83% of patients, respectively. The combination of data from both modalities achieved a combined diagnostic accuracy of 90% (correct diagnosis in 26 of 29 patients).<sup>30</sup>

### cMRI in Treatment Selection and Monitoring

Traditionally, RHC has been used to diagnose and assess vasoreactivity to help determine initial treatment selection. Vasodilator response may also provide prognostic information with regard to the extent of vascular remodeling and retained cardiac function. A pilot study in 19 PAH patients shortly after RHC showed that MRI assessment of main pulmonary artery distensibility was highly correlated with vasodilator response ( $P = 0.01$ ).<sup>31</sup> A cutoff value of 10% distensibility enabled responders to be distinguished from nonresponders with 100% sensitivity and 56% specificity. To date, it has been difficult to correlate functional improvement with improvement in hemodynamic parameters in PAH clinical studies. Roeleveld and colleagues<sup>32</sup> performed cMRI in 11 PAH patients receiving continuous intravenous epoprostenol to assess increase in RV stroke volumes. They showed that the most significant improvement in RV stroke volume was observed during the first 4 months of treatment and was closely correlated with increase in 6-min walk distance. Van Wolferen and colleagues<sup>33</sup> investigated relationship between right ventricular structure and function to survival in idiopathic pulmonary arterial hypertension. A trend of increasing RV volume, decreasing stroke volume and LV volume are strong predictors of mortality and treatment failure.

Finally, MRI has been used to show restoration of the RV structure and function after pulmonary endarterectomy in patients with CTEPH.<sup>34</sup> Before surgery, there were significant differences between patients with CTEPH and healthy controls in right ventricular volumes, LV end-diastolic volume, RV mass, and leftward ventricular septal bowing. After at least 4 months post-surgery, pulmonary hemodynamics improved in the 17 patients and normalization occurred in the following measures: RV and LV volumes and leftward ventricular septal bowing. Thus, MRI was able to evaluate cardiac remodeling in CTEPH patients and to demonstrate restoration of the RV after pulmonary endarterectomy.

## Limitations

MRI is still expensive and not widely available. Certain contraindications may preclude universal use of MRI: these include inability to perform breath hold, claustrophobia and MRI incompatible hardware such as neurostimulators, cochlear implants, aneurysm clips, etc.

Even with the improved imaging parameters, the diagnostic accuracy of high-spatial-resolution MR angiography is limited in demonstrating pathologic findings that affect more peripheral territories of pulmonary vasculature and in facilitating the diagnosis of smaller and older organized thrombi. In particular, the sensitivity of MR angiography compared with that of DSA or CT angiography was rather low for the detection of the corkscrew phenomenon, as well as for the detection of webs and bands at the subsegmental level.<sup>30</sup> A comparison between state-of-the-art MR angiography and multidetector row CT angiography of the pulmonary vasculature shows that multidetector row CT angiography still seems superior with regard to ease of use, short acquisition time, and high spatial resolution. These factors make CT angiography the modality of choice in acute settings like detection of pulmonary embolism.

## Future Directions

### MRI perfusion imaging of pulmonary parenchyma

Since the current emphasis of PAH therapeutics is to reverse the proliferative remodeling or regenerate the pulmonary circulation, molecular imaging end points will become increasingly relevant in the assessment of these patients. For example, promising vascular proapoptotic therapies will require a means of anatomic and functional imaging of the pulmonary circulation.<sup>35-37</sup>

Magnetic resonance imaging of pulmonary parenchyma has been hampered by the extremely heterogeneous magnetic susceptibility of lung due to multiple air-tissue interfaces.<sup>38</sup> In addition, intrinsic low proton spin density, respiration and cardiac motion, pulmonary blood flow and molecular diffusion also attribute to the low MR signal intensity of pulmonary parenchyma.<sup>39</sup> Recently, improvements in MRI techniques have widened the potential for investigation of pulmonary parenchyma by performing ventilation and perfusion imaging.<sup>40</sup> Methodologically, perfusion imaging includes two basic approaches<sup>41</sup>: arterial spin labeling (ASL) and dynamic contrast-enhanced imaging. Arterial spin labeling is a relatively new technique for MRI perfusion imaging. It does not require injection of contrast agents, and uses magnetically labeled blood water as an endogenous, freely diffusible tracer; hence it is completely noninvasive. Dynamic contrast-enhanced magnetic resonance imaging has long been proposed for the assessment of lung perfusion, which is based on the contrast enhancement of pulmonary parenchyma during the first pass of a bolus of contrast agent through the pulmonary circulation.<sup>41</sup> In order to display small perfusion defects at the lung periphery, high spatial resolution is required. Combined with parallel imaging, which can reduce the acquisition time and improve the temporal

**Table. Comparison of cMRI, RHC, and Echocardiography in Pulmonary Hypertension**

Parameter	Modality		
	Cardiac MRI	Echocardiography (Including 3-dimensional echocardiography)	RHC (including Right-sided angiocardiology)
<b>RV assessment</b>			
Volumes	+++	++	+
Ejection fraction	+++	++	+
Strain	+++	++	-
RV pressure	-/+	++	+++
Stroke volume	+++	+	+++
Mass	++	-/+	-
RV remodeling including septal curvature	+++	++	-
Tricuspid regurgitation	++	+++	+
Miscellaneous (pericardial effusion, pulmonary embolism, and other incidental findings)	++	+	+
<b>RA assessment</b>			
RA pressure	-	-	+++
<b>PA dimensions</b>			
PA distensibility	+++	+	-/+
PA hemodynamics	-/+	+	+++
Quantitative lung flow	+++	-	-

\*Ideally invasive MRI (ie, simultaneous evaluation of MRI-derived volume and flow parameters with RHC derived pressure measurements) may be the most accurate method of assessing cardiac hemodynamics.

-, not useful; +, may be useful; ++, useful; +++, extremely useful; MRI, magnetic resonance imaging; PA, pulmonary artery; RA, right atria; RHC, right heart catheterization; RV, right ventricle.

resolution, 3D breath-hold dynamic contrast-enhanced imaging is feasible for the assessment of pulmonary parenchyma

### MRI-Guided Catheterization

MRI alone has limited ability to assess load-independent parameters of ventricular function (such as myocardial contractility) in PH. A novel hybrid technique, real-time MRI-guided catheterization, uses MRI guided catheterization to combine pressure time loops obtained by catheter and volume-time loops obtained from cMRI.<sup>42</sup> Therefore pressure volume loops are created, from which some of the important mechanical parameters can be obtained.

Kuehne and colleagues<sup>43</sup> showed the ability of MRI-guided catheterization to construct RV pressure-volume loops, and in turn to calculate RV afterload, myocardial contractility, pump function, and RV-pulmonary artery coupling in healthy volunteers and PAH patients. Despite significantly greater myocardial contractility among PAH patients, RV pump function was compromised compared with healthy volunteers, in part because of inefficient coupling between the RV and pulmonary circulation. In a second study, Kuehne and colleagues<sup>44</sup> showed that PVR assessment using MRI-guided catheterization and MRI velocity mapping provided more reproducible results than the traditional thermodilution method. In addition, this technique seems to provide the ability to sample PVR more comprehensively (including both overall and branch-specific resistance) than can be achieved using Doppler guidewires.

### Summary of Utility of MRI in Characterizing PH

Currently, right heart catheterization and echocardiography are the primary tools used in the diagnosis and monitoring of PH. cMRI has already replaced echocardiography and other tools as a reference standard for the non-invasive evaluation of RV structure and function that is integral to PH. The **Table** summarizes comparison of the usefulness of the different imaging modalities and

RHC in PH.<sup>45</sup> An ongoing multicenter clinical trial (COMPASS3) should provide pivotal information for the use of cMRI derived parameters in PH.<sup>46</sup> Emerging applications and advancement will result in an even greater role of cMRI in the future for developing personalized approaches in the management of PH.

## References

1. Simonneau G, Galie N, Rubin LJ, et al. Clinical classification of pulmonary hypertension. *J Am Coll Cardiol*. June 16, 2004;43(12\_Suppl\_S):5S-12.
2. Barst RJ, McGoon M, Torbicki A, et al. Diagnosis and differential assessment of pulmonary arterial hypertension. *J Am Coll Cardiol*. June 16, 2004;43(12\_Suppl\_S):40S-47.
3. Galie N, Torbicki A, Barst R, et al. Guidelines on diagnosis and treatment of pulmonary arterial hypertension. The Task Force on Diagnosis and Treatment of Pulmonary Arterial Hypertension of the European Society of Cardiology. *Eur Heart J*. Dec 2004;25(24):2243-2278.
4. Galie N, Manes A, Branzi A. Evaluation of pulmonary arterial hypertension. *Curr Opin Cardiol*. Nov 2004;19(6):575-581.
5. Finn JP, Nael K, Deshpande V, et al. Cardiac MR Imaging: State of the Technology. *Radiology*. November 1, 2006;241(2):338-354.
6. Dias CA, Assad RS, Caneo LF, et al. Reversible pulmonary trunk banding. II. An experimental model for rapid pulmonary ventricular hypertrophy. *J Thorac Cardiovasc Surg*. November 1, 2002;124(5):999-1006.
7. McLaughlin VV, Sitbon O, Badesch DB, et al. Survival with first-line bosentan in patients with primary pulmonary hypertension. *Eur Respir J*. February 1, 2005;25(2):244-249.
8. Sandoval J, Bauerle O, Palomar A, et al. Survival in primary pulmonary hypertension. Validation of a prognostic equation. *Circulation*. April 1, 1994;89(4):1733-1744.
9. D'Alonzo GE, Barst RJ, Ayres SM, et al. Survival in patients with primary pulmonary hypertension. Results from a national prospective registry. *Ann Intern Med*. Sep 1 1991;115(5):343-349.
10. Mogelvang J, Stubgaard M, Thomsen C, et al. Evaluation of right ventricular volumes measured by magnetic resonance imaging. *Eur Heart J*. May 1, 1988;9(5):529-533.
11. Tandri H, Daya SK, Nasir K, et al. Normal Reference Values for the Adult Right Ventricle by Magnetic Resonance Imaging. *The American Journal of Cardiology*. 2006;98(12):1660-1664.
12. Lorenz CH, Walker ES, Graham TP, Jr., et al. Right Ventricular Performance and Mass by Use of Cine MRI Late After Atrial Repair of Transposition of the Great Arteries. *Circulation*. November 1, 1995;92(9):233-239.
13. Grothues F, Moon JC, Bellenger NG, et al. Interstudy reproducibility of right ventricular volumes, function, and mass with cardiovascular magnetic resonance. *American Heart Journal*. 2004;147(2):218-223.
14. Tanaka H, Tei C, Naka S, et al. Diastolic bulging of the interventricular septum toward the left ventricle. An echocardiographic manifestation of negative interventricular pressure gradient between left and right ventricles during diastole. *Circulation*. September 1, 1980;62(3):558-563.
15. Marcus JT, Gan CT-J, Zwaneburg JJM, et al. Interventricular Mechanical Asynchrony in Pulmonary Arterial Hypertension: Left-to-Right Delay in Peak Shortening Is Related to Right Ventricular Overload and Left Ventricular Underfilling. *J Am Coll Cardiol*. February 19, 2008;51(7):750-757.
16. DelleGrottaglie S, Sanz J, Poon M, et al. Pulmonary Hypertension: Accuracy of Detection with Left Ventricular Septal-to-Free Wall Curvature Ratio Measured at Cardiac MR. *Radiology*. April 1, 2007;243(1):63-69.
17. Laffon E, Vallet C, Bernard V, et al. A computed method for noninvasive MRI assessment of pulmonary arterial hypertension. *J Appl Physiol*. February 1, 2004;96(2):463-468.
18. Roeleveld RJ, Marcus JT, Boonstra A, et al. A comparison of noninvasive MRI-based methods of estimating pulmonary artery pressure in pulmonary hypertension. *J Magn Reson Imaging*. Jul 2005;22(1):67-72.
19. Saba TS, Foster J, Cockburn M, et al. Ventricular mass index using magnetic resonance imaging accurately estimates pulmonary artery pressure. *Eur Respir J*. December 1, 2002;20(6):1519-1524.
20. Sanz J, Kuschnir P, Rius T, et al. Pulmonary Arterial Hypertension: Non-invasive Detection with Phase-Contrast MR Imaging. *Radiology*. April 1, 2007;243(1):70-79.
21. Kondo C, Caputo GR, Masui T, et al. Pulmonary hypertension: pulmonary flow quantification and flow profile analysis with velocity-encoded cine MR imaging. *Radiology*. June 1, 1992;183(3):751-758.
22. Ley S, Mereles D, Puderbach M, et al. Value of MR phase-contrast flow measurements for functional assessment of pulmonary arterial hypertension. *European Radiology*. 2007;17(7):1892-1897.
23. Blyth KG, Groenning BA, Martin TN, et al. Contrast enhanced-cardiovascular magnetic resonance imaging in patients with pulmonary hypertension. *Eur Heart J*. October 1, 2005;26(19):1993-1999.
24. McCann GP, Gan CT, Beek AM, et al. Extent of MRI Delayed Enhancement of Myocardial Mass Is Related to Right Ventricular Dysfunction in Pulmonary Artery Hypertension. *Am J Roentgenol*. February 1, 2007;188(2):349-355.
25. Gan CT-J, Holverda S, Marcus JT, et al. Right Ventricular Diastolic Dysfunction and the Acute Effects of Sildenafil in Pulmonary Hypertension Patients. *Chest*. July 1, 2007;132(1):11-17.
26. McLaughlin VV, Presberg KW, Doyle RL, et al. Prognosis of Pulmonary Arterial Hypertension\*: ACCP Evidence-Based Clinical Practice Guidelines. *Chest*. July 1, 2004;126(1\_suppl):78S-92.
27. Michelakis ED. Spatio-Temporal Diversity of Apoptosis Within the Vascular Wall in Pulmonary Arterial Hypertension: Heterogeneous BMP Signaling May Have Therapeutic Implications. *Circ Res*. February 3, 2006;98(2):172-175.
28. Dartevelle P, Fadel E, Mussot S, et al. Chronic thromboembolic pulmonary hypertension. *Eur Respir J*. April 1, 2004;23(4):637-648.
29. Ryan KL, Fedullo PF, Davis GB, et al. Perfusion scan findings understate the severity of angiographic and hemodynamic compromise in chronic thromboembolic pulmonary hypertension. *Chest*. June 1, 1988;93(6):1180-1185.
30. Nikolaou K, Schoenberg SO, Attenberger U, et al. Pulmonary Arterial Hypertension: Diagnosis with Fast Perfusion MR Imaging and High-Spatial-Resolution MR Angiography—Preliminary Experience. *Radiology*. August 1, 2005;236(2):694-703.
31. Jardim C, Rochitte CE, Humbert M, et al. Pulmonary artery distensibility in pulmonary arterial hypertension: a MRI pilot study. *Eur Respir J*. November 29, 2006;28(11):2006-09031936.00016806.
32. Roeleveld RJ, Vonk-Noordegraaf A, Marcus JT, et al. Effects of Epoprostenol on Right Ventricular Hypertrophy and Dilatation in Pulmonary Hypertension. *Chest*. February 2004;125(2):572-579.
33. van Wolferen SA, Marcus JT, Boonstra A, et al. Prognostic value of right ventricular mass, volume, and function in idiopathic pulmonary arterial hypertension. *Eur Heart J*. May 2, 2007;28(10):1250-1257.
34. Reesink HJ, Marcus JT, Tulevski II, et al. Reverse right ventricular remodeling after pulmonary endarterectomy in patients with chronic thromboembolic pulmonary hypertension: Utility of magnetic resonance imaging to demonstrate restoration of the right ventricle. *The Journal of Thoracic and Cardiovascular Surgery*. 2007;133(1):58-64.
35. Cowan KN, Heilbut A, Humpl T, et al. Complete reversal of fatal pulmonary hypertension in rats by a serine elastase inhibitor. *Nat Med*. Jun 2000;6(6):698-702.
36. McMurtry MS, Archer SL, Altieri DC, et al. Gene therapy targeting survivin selectively induces pulmonary vascular apoptosis and reverses pulmonary arterial hypertension. *J Clin Invest*. Jun 2005;115(6):1479-1491.
37. McMurtry MS, Bonnet S, Wu X, et al. Dichloroacetate Prevents and Reverses Pulmonary Hypertension by Inducing Pulmonary Artery Smooth Muscle Cell Apoptosis. *Circ Res*. October 15, 2004;95(8):830-840.
38. Hatabu H, Chen Q, Stock KW, et al. Fast magnetic resonance imaging of the lung. *Eur J Radiol*. Feb 1999;29(2):114-132.
39. Bergin CJ, Glover GM, Pauly J. Magnetic resonance imaging of lung parenchyma. *J Thorac Imaging*. Winter 1993;8(1):12-17.
40. Mills GH, Wild JM, Eberle B, et al. Functional magnetic resonance imaging of the lung. *Br J Anaesth*. Jul 2003;91(1):16-30.
41. Uematsu H, Levin DL, Hatabu H. Quantification of pulmonary perfusion with MR imaging: recent advances. *Eur J Radiol*. Mar 2001;37(3):155-163.
42. Lederman RJ. Cardiovascular Interventional Magnetic Resonance Imaging. *Circulation*. November 8, 2005;112(19):3009-3017.
43. Kuehne T, Yilmaz S, Steendijk P, et al. Magnetic Resonance Imaging Analysis of Right Ventricular Pressure-Volume Loops: In Vivo Validation and Clinical Application in Patients With Pulmonary Hypertension. *Circulation*. October 5, 2004;110(14):2010-2016.
44. Kuehne T, Yilmaz S, Schulze-Neick I, et al. Magnetic resonance imaging guided catheterisation for assessment of pulmonary vascular resistance: in vivo validation and clinical application in patients with pulmonary hypertension. *Heart*. August 1, 2005;91(8):1064-1069.
45. Benza R, Biederman R, Murali S, et al. Role of Cardiac Magnetic Resonance Imaging in the Management of Patients With Pulmonary Arterial Hypertension. *J Am Coll Cardiol*. November 18, 2008;52(21):1683-1692.
46. Gupta H, Desai R, Torres F, Soto F, Park M, McQueen C, Murali S, Benza R. Right Ventricular Mass Index Predicts Pulmonary Vascular Resistance in Pulmonary Arterial Hypertension: Baseline Cardiac MRI Results of the COMPASS-3 Abstract accepted for Oral Presentation at: American College of Cardiology, 2009; Orlando. ■